Influence of low concentrations of scatterers and signal detection time on the results of their measurements using dynamic light scattering

N.F. Bunkin, A.V. Shkirin, N.V. Suyazov, L.L. Chaikov,
S.N. Chirikov, M.N. Kirichenko, S.D. Nikiforov, S.I. Tymper

Abstract. **The influence of limited detection time on the form of the autocorrelation function (ACF) has been analysed for measurements in low-concentration suspensions by dynamic light scattering with allowance for the spatial distribution of the laser beam intensity. The general view of the ACF of the scattered light intensity is obtained for a Gaussian beam and a finite measurement time. The results of the theoretical analysis are compared with the experimental data and the results obtained by computer simulation of the scattering from an ensemble of particles involved in Brownian motion in a Gaussian beam. It is shown that, in the case of low suspension concentrations, the ACF distortions related to finite detection time lead to underestimation of the particle sizes and occurrence of an artefact peak in the distribution of the scattered light intensity over scatterer sizes. An empirical dependence of the measured size of particles on their number in the scattering volume is found.**

1. Introduction

Currently, dynamic light scattering (DLS) is widely used for contactless and rapid (measurement time of 10–100 s) determination of the sizes of nanoparticles and macromolecules in liquids [1–4].

N.F. Bunkin A.M. Prokhorov General Physics Institute, Russian Academy of Sciences, ul. Vavilova 38, 119991 Moscow, Russia;
N.E. Bauman Moscow State Technical University, Vtoraya Baumanskaya ul. 5, 105005 Moscow, Russia;
e-mail: nbunkin@kapella.gpi.ru;
A.V. Shkirin A.M. Prokhorov General Physics Institute, Russian Academy of Sciences, ul. Vavilova 38, 119991 Moscow, Russia;
National Research Nuclear University 'MEPhI', Kashirskoe sh. 31, 115409 Moscow, Russia; e-mail: avshkirin@mephi.ru;
N.V. Suyazov A.M. Prokhorov General Physics Institute, Russian Academy of Sciences, ul. Vavilova 38, 119991 Moscow, Russia;
e-mail: nvsnvs@list.ru
L.L. Chaikov P.N. Lebedev Physical Institute, Russian Academy of Sciences, Leninsky prosp. 53, 119991 Moscow, Russia; National Research Nuclear University 'MEPhI', Kashirskoe sh. 31, 115409 Moscow, Russia; e-mail: chaik@sci.lebedev.ru;
S.N. Chirikov, S.D. Nikiforov, S.I. Tymper National Research Nuclear University 'MEPhI', Kashirskoe sh. 31, 115409 Moscow, Russia; e-mail: snchirikov@mephi.ru, sitymper@mephi.ru;
M.N. Kirichenko P.N. Lebedev Physical Institute, Russian Academy of Sciences, Leninsky prosp. 53, 119991 Moscow, Russia; e-mail: kirmari@sci.lebedev.ru

The accuracy of the results obtained by this method depends on a number of factors, which include correct selection of the scattering volume for detecting spatially coherent scattered light, the possibility of interaction between nanoparticles and the dependence of the diffusion coefficient on their concentration, the validity of single-scattering condition, and the presence of foreign sources of scattered light (for example, large impurity particles). Among the factors affecting the DLS data, we should note the inhomogeneous illumination of the scattering volume (which is related to the spatial distribution of laser beam intensity) and violation of the Gaussian field statistics at a small number of particles in this volume [5–7]. These factors were considered as a source of the artefact peak in the distribution of the scattered light intensity over scattering-particle sizes in highly diluted samples [5–7]. This feature becomes important when the object of study is low-concentration and polydisperse suspensions. When analysing the aforementioned factors, it is of key importance to take into account the finiteness of measurement time. In this paper, we report the results of studying the influence of this finiteness on the form of the autocorrelation function (ACF) for low-concentration suspensions.

2. Theory

At low scatterer concentrations, when the number of particles in the scattering volume ranges from one to ten, the statistics of scattered-light-field fluctuations significantly differs from Gaussian [8, 9]. The motion of each particle becomes important, and the effect of particle 'input–output' from the scattering volume manifests itself and contributes to the ACF of the scattered light intensity measured by the DLS method. In the case of a limited scattering region, the time dependence of the ACF is determined by two mechanisms, whose contributions are generally characterised by significantly different correlation times. The smaller time scale is related to the change in the phase of the field scattered by a moving Brownian particle, while the larger scale is determined by the fluctuations of the number of Brownian particles in the effective scattering volume [8]. In addition, the limited signal detection time leads to additional distortions when processing DLS data. Below we will consider the influence of the detection time finiteness on the intensity ACF obtained by the DLS method with allowance for the limited effective scattering volume; the consideration will be performed within the model of Gaussian distribution of the probe light intensity in space, which is convenient for analytical calculations.

The light incident on a dispersed system can be presented as a plane wave propagating along the *z* axis, whose amplitude decreases with increasing distance in the transverse

direction according to the Gaussian law with a parameter a (approximate model of the field in the Gaussian beam waist):

$$
E_{in}(x,y,z) = A_0 \exp\left(i\omega t - ikz - \frac{x^2+y^2}{a^2}\right)
$$
$$
+ A_0^* \exp\left(-i\omega t + ikz - \frac{x^2+y^2}{a^2}\right). \tag{1}
$$

We assume that the limitation of the scattering region size along the z axis, which is determined by the detecting system aperture and the waist length, can be modelled by a Gaussian dependence $\exp(-z^2/b^2)$ with a parameter b.

Then, at a large distance r from the centre of the scattering region ($r \gg kb^2, ka^2, b, a$), the field $E_j(t)$ scattered by the jth particle, located at the point $r_j(t) = [x_j(t), y_j(t), z_j(t)]$ at an instant t, can be written as

$$
E_j(t) = F_j(t)\exp(i\omega t - ikr) + F_j^*(t)\exp(-i\omega t + ikr). \tag{2}
$$

In this relation,

$$
F_j(t) = A_0 \frac{f(\theta)}{r} U(r_j(t))\exp[iqr_j(t)], \tag{3}
$$

where $q = [q_x, q_y, q_z]$ is the scattering vector and

$$
U(r_j(t)) = \exp\left[-\frac{x_j^2(t)+y_j^2(t)}{a^2} - \frac{z_j^2(t)}{b^2}\right]
$$

is the dimensionless amplitude of the wave exciting scattering at the jth-particle location point. Let the detecting system be placed in the xz plane and accept light scattered at an angle θ with respect to the incident beam direction; then, the scattering vector has only two nonzero components: $q_x = k\sin\theta$ and $q_z = k(\cos\theta - 1)$. The quantity $f(\theta)$ in (3) is the scattering amplitude, which is related to the differential scattering cross section $\sigma(\theta)$ (scattering cross section into unit solid angle) as follows: $\sigma(\theta) = |f(\theta)|^2$. The field scattered by N particles has the form

$$
E(t) = \sum_{j=1}^{N} E_j(t),
$$

and the correlation function of the light intensity scattered by all these particles can be written as

$$
G^{(2)}(\tau) = \langle E^2(t)E^2(t+\tau)\rangle
$$
$$
= \sum_{j_1,j_2,j_3,j_4=1}^{N} \langle E_{j_1}(t)E_{j_2}(t)E_{j_3}(t+\tau)E_{j_4}(t+\tau)\rangle, \tag{4}
$$

where the angle brackets denote averaging over an ensemble of particles. Let us substitute expression (2) into sum (4) and reject all rapidly oscillating (with optical frequency ω and frequencies multiple of it) terms:

$$
G^{(2)}(\tau) = 4 \sum_{j_1,j_2,j_3,j_4=1}^{N} \langle F_{j_1}(t)F_{j_2}^*(t)F_{j_3}(t+\tau)F_{j_4}^*(t+\tau)\rangle. \tag{5}
$$

Let scattering particles with a radius R undergo independently Brownian motion with a diffusion coefficient D. The joint probability density for a particle to be at point $r_j(t)$ at the

instant t and at point $r_j(t+\tau)$ at the instant $t+\tau$ can be written as (see, e.g., [10–12])

$$
p_2(r_j(t),r_j(t+\tau)) = (4\pi D\tau)^{-3/2}
$$
$$
\times \exp\left[-\frac{(r_j(t+\tau)-r_j(t))^2}{4D\tau}\right]p_1, \tag{6}
$$

where $\tau > 0$; p_1 is the single-point probability density for a particle to occupy a specified point with coordinates r, which is independent of time and coordinates r_j ($p_1 = \mathrm{const}$) in the case of stationary Brownian motion. Using the statistical independence of the Brownian motion of individual particles, one can write the probability density for N particles as the product of N probabilities in form (6). Now, with allowance for the Gaussian description of the scattering region (3), the averaging for calculating correlation function (5) can be performed explicitly. In a typical experimental situation, when the scattering region sizes are sufficiently large in comparison with the light wavelength [$aq_x, bq_z \gg 1, (\ln\eta)^{1/2}$], the expression derived for $G^{(2)}(\tau)$ can be simplified by rejecting exponentially small terms (η is the average number of particles in the scattering region). We assume also that the total number of particles in the system under consideration (the cell with a sample) is $N \gg 1$. Then the intensity correlation function can be written as

$$
G^{(2)}(\tau) = \frac{I_0^2 \sigma^2(\theta)}{R^4}\eta^2
$$
$$
\times \left\{ 1 + \frac{a^4 b^2 \exp\left(-\dfrac{2a^2 q_x^2 D|\tau|}{2D|\tau|+a^2} - \dfrac{2b^2 q_z^2 D|\tau|}{2D|\tau|+b^2}\right)}{(2D|\tau|+a^2)^2 (2D|\tau|+b^2)} \right.
$$
$$
\left. + \frac{a^2 b}{2^{3/2}\eta(4D|\tau|+a^2)\sqrt{4D|\tau|+b^2}} \right\}, \tag{7}
$$

where $I_0 = 2|A|_0^2$ is the incident wave intensity at the beam centre;

$$
\eta = nV_s; \tag{8}
$$

$V_s = (\pi/2)^{3/2}a^2 b$ is the effective volume of scattering region and $n = Np_1$ is the average particle concentration. Under typical conditions of the DLS experiment, the second term in the braces in (7) is not vanishingly small in comparison with unity only when the following strong inequality is satisfied: $D|\tau| \ll a^2, b^2$. In this case, the ACF of the recorded intensity can be simplified and written in the form

$$
G^{(2)}(\tau) = \frac{I_0^2 \sigma^2(\theta)}{r^4}\eta^2
$$
$$
\times \left\{ 1 + \exp(-2q^2 D|\tau|) + \frac{a^2 b}{2^{3/2}\eta(4D|\tau|+a^2)\sqrt{4D|\tau|+b^2}} \right\}, \tag{9}
$$

where $q = \sqrt{q_z^2 + q_x^2} = 2k\sin(\theta/2)$.

Without the last (third) term in the braces, formula (9) describes the conventional ACF for infinite scattering region and independence of the incident plane wave amplitude on coordinates: $U(r_k) \equiv 1$. In this case, the expression in the braces takes a well-known form:

$$1 + \exp(-2q^2 D|\tau|). \qquad (10)$$

Note that the necessity of taking into account the spatial coherence of the scattered light in experiments [13] lead to the occurrence of a constant (spatial coherence) factor γ before $\exp(-2q^2 D|\tau|)$ in expression (10), which is determined by the optical system geometry.

The third term in the braces in formula (9), related to the limited size of the scattering region, is important when the number of particles in the scattering volume is small. It is proportional to the ACF of fluctuations of the number of Brownian particles present in the scattering region [14, 15].

Relation (9) can also be generalised to the case of scattering by particles with different sizes, and therefore, different diffusion coefficients and scattering cross sections:

$$G^{(2)}(\tau) = \frac{I_0^2}{r^4}\Bigg\{\Big(\sum_l \eta_l \sigma_l(\theta)\Big)^2 + \Big(\sum_l \eta_l \sigma_l(\theta)\exp(- q^2 D_l |\tau|)\Big)^2$$

$$+ \sum_l \frac{\eta_l \sigma_l^2(\theta) a^2 b}{2^{3/2}(4D_l|\tau|+ a^2)\sqrt{4D_l|\tau|+ b^2}}\Bigg\}, \qquad (11)$$

where $\eta_l = V_s n_l$; n_l is the average concentration of particles with a diffusion coefficient D_l and differential cross section $\sigma_l(\theta)$.

The detection time T in measurements should satisfy the condition $T \gg (2q^2 D)^{-1}$, where $(2q^2 D)^{-1}$ is the correlation time, determined by the Brownian diffusion. With an increase in τ, the second term in (9) decreases to values close to the third term. Therefore, $G^{(2)}(\tau)$ at low particle concentrations in a finite scattering region differs from the $G^{(2)}(\tau)$ value for an infinite scattering region; this circumstance affects the results of reconstructing the particle-size distribution.

Note that the limited detection time may lead to distortions of $G^{(2)}(\tau)$ for the following reason. When processing DLS data, the $G^{(2)}(\tau)$ value is found by averaging the scattering intensity over the experimental realisation time on a finite interval of duration T. In this case,

$$\lim_{\tau \to \infty} G^{(2)}(\tau) \equiv G^{(2)}(\infty) = \bar{I}^2 \approx \Big(\frac{1}{T}\int_0^T I(t)\,\mathrm{d}t\Big)^2 \qquad (12)$$

is the so-called baseline, where $I(t)$ is the recorded scattered light intensity. The experimentally found ACF intensity has the form

$$G_{\exp}^{(2)}(\tau) = \frac{1}{T-\tau}\int_0^{T-\tau} I(t)I(t+\tau)\,\mathrm{d}t - \Big(\frac{1}{T}\int_0^T I(t)\,\mathrm{d}t\Big)^2. \quad (13)$$

It should be emphasised that $G_{\exp}^{(2)}(\tau)$ theoretically corresponds to $G^{(2)}(\tau) - G^{(2)}(\infty)$ rather than to $G^{(2)}(\tau)$. In order to relate the experimental correlation function $G_{\exp}^{(2)}(\tau)$, found above by averaging over time, with the ACF $G^{(2)}(\tau)$ obtained by averaging over the ensemble, we will apply averaging over the ensemble to equality (13). Based on the suggested ergodicity of the scattered field (and the interpretation of averaging over an ensemble as averaging over different realisations of particle arrangement, which is often used in practice), one can conclude that, for sufficiently large averaging intervals $T - \tau$, the ensemble-averaged function $\langle G_{\exp}^{(2)}(\tau)\rangle$ will not significantly differ from the function $G_{\exp}^{(2)}(\tau)$ calculated based on the experimental data. Having denoted the $\langle G_{\exp}^{(2)}(\tau)\rangle$ value obtained by averaging formula (13) over an ensemble as

$G_{th}^{(2)}(\tau)$, we arrive at the following expression for the ACF at a finite measurement time T:

$$G_{th}^{(2)}(\tau) \equiv \langle G_{\exp}^{(2)}(\tau)\rangle = G^{(2)}(\tau) - B_{th}(T), \qquad (14)$$

where

$$B_{th}(T) = \frac{1}{T^2}\int_0^T\int_0^T G^{(2)}(t' - t'')\,\mathrm{d}t'\,\mathrm{d}t''$$

is the theoretical estimate of the baseline $[G^{(2)}(\infty)]$ with allowance for the finite measurement time. The 'distortions' of the experimentally found ACF intensity, related to the limited detection time, are described by the second term in (14). These distortions depend on the ACF form. Having substituted (9) into (14), one can obtain an explicit analytical expression for approximating the experimentally found intensity ACF:

$$G_{th}^{(2)}(\tau) = \frac{I_0^2 \sigma^2(\theta)}{r^4}\eta^2 \Bigg\{\exp(-\tau_D) - \frac{2[T_D - 1 + \exp(-T_D)]}{T_D^2}$$

$$+ \frac{a_q^2 b_q}{2^{3/2}\eta(\tau_D + a_q^2)\sqrt{\tau_D + b_q^2}} + \frac{\sqrt{2}\, a_q^2 b_q}{\eta T_D^2}\Bigg[\sqrt{b_q^2 + T_D} - b_q$$

$$+ \frac{(a_q^2 + T_D)\Big(\mathrm{arcoth}\,\sqrt{\frac{b_q^2 - a_q^2}{b_q^2 + T_D}} - \mathrm{arcoth}\,\frac{\sqrt{b_q^2 - a_q^2}}{b_q}\Big)}{\sqrt{b_q^2 - a_q^2}}\Bigg]\Bigg\}, \quad (15)$$

where

$$\tau_D = 2Dq^2\tau, \quad T_D = 2Dq^2 T, \quad a_q = \frac{aq}{\sqrt{2}}, \quad b_q = \frac{bq}{\sqrt{2}} \qquad (16)$$

are, respectively, the normalised values of the correlation function argument, the detection time, and the scattering region sizes.

In two characteristic limiting cases of the size ratio for the scattering region, when $b = a$ (the longitudinal size of this region, determined by the detecting system aperture, is equal to the beam width) and $b \gg a$, formula (15) takes the form

$$G_{th}^{(2)}(\tau)\big|_{b = a} = \frac{I_0^2 \sigma^2(\theta)}{r^4}\eta^2 \Bigg\{\exp(-\tau_D) - \frac{2[T_D - 1 + \exp(-T_D)]}{T_D^2}$$

$$+ \frac{a_q^3}{2^{3/2}\eta(\tau_D + a_q^2)^{3/2}} + \frac{\sqrt{2}\, a_q^2\big(2a_q\sqrt{a_q^2 + T_D} - T_D - 2a_q^2\big)}{\eta T_D^2}\Bigg\}, \quad (17)$$

$$G_{th}^{(2)}(\tau)\big|_{b \gg a} = \frac{I_0^2 \sigma^2(\theta)}{r^4}\eta^2 \Bigg\{\exp(-\tau_D) - \frac{2[T_D - 1 + \exp(-T_D)]}{T_D^2}$$

$$+ \frac{a_q^2}{2^{3/2}\eta(\tau_D + a_q^2)} + \frac{a_q^2\Big[(a_q^2 + T_D)\ln\Big(\frac{a_q^2}{a_q^2 + T_D}\Big) + T_D\Big]}{\sqrt{2}\,\eta T_D^2}\Bigg\}. \quad (18)$$

To verify the above-formulated theoretical model, which takes into account the correction to the finite detection time, we performed a computer simulation of the motion dynamics for a finite number of Brownian particles obeying the Smoluchowski–Einstein statistics and numerically calculated the time dependence of scattered light intensity on the interval $[0, T]$, along with its ACF. The simulation was performed within the MatLab environment. During the simulation, a set

of random realisations, corresponding to a specified number N of particles and their initial positions in space, was generated. The initial positions of particles were set as random and uniformly distributed. The recorded intensity of the scattered light, accurate to the time-independent factor, was found from the equality

$$I(t) \sim EE^*$$ (19)

$$= \left| \sum_{j=1}^{N} U(x_j(t), y_j(t), z_j(t)) \exp\{-i[q_x x_j(t) + q_z z_j(t)]\} \right|^2,$$

where $x_j(t)$, $y_j(t)$, and $z_j(t)$ are time-dependent coordinates of the jth Brownian particle. The function

$$U(x, y, z) = \exp\left[-\left(\frac{x^2}{a_x^2} + \frac{y^2}{a_y^2} + \frac{z^2}{a_z^2} \right) \right],$$ (20)

which describes the excitation-wave form, in fact modelled the region of recorded scattering. The Gaussian parameters of the scattering volume, a_x, a_y, and a_z, were determined by both the beam sizes and the geometry of the detecting optical system. We considered the case where, as well as in formulas (7) and (9), $a_x = a_y = a$ and $a_z = b$ (i.e., this region is limited in the transverse directions by the Gaussian beam width a). The limitation in the longitudinal direction (along the z axis) is modelled by a Gaussian dependence with a parameter b; for the effective size of detection aperture b_0 and scattering at an angle θ, this parameter can be estimated from the relation $b = b_0/\sin\theta$.

Within the MatLab environment, the intensity ACF $K(\tau)$ is determined by averaging the product of increments $\Delta I(t) \times \Delta I(t + \tau)$ over time on the interval $[0, T]$:

$$K(\tau) = \frac{1}{T} \int_0^{T-\tau} \left[I(t) - \frac{1}{T} \int_0^T I(t') \mathrm{d}t' \right]$$

$$\times \left[I(t + \tau) - \frac{1}{T} \int_0^T I(t'') \mathrm{d}t'' \right] \mathrm{d}t.$$ (21)

As in derivation of (14), we will apply averaging over an ensemble to equality (21):

$$K_{\text{th}}(\tau) \equiv \langle K(\tau) \rangle = \frac{T - \tau}{T} G^{(2)}(\tau) - \frac{T + \tau}{T^3}$$

$$\times \int_0^T \int_0^T G^{(2)}(t' - t'') \mathrm{d}t' \mathrm{d}t'' + \frac{2}{T^2} \int_0^\tau \int_0^T G^{(2)}(t' - t'') \mathrm{d}t' \mathrm{d}t''.$$ (22)

The ACF $K(\tau)$, obtained by numerical simulation, is approximately equal to $K_{\text{th}}(\tau)$ on the assumption of the scattered field ergodicity.

The distortions of the intensity ACF in (22) that are due to the limited detection time are described mainly by the second and third terms. Having substituted the function $G^{(2)}(\tau)$ from (9) into (22), one can obtain an explicit expression for $K_{\text{th}}(\tau)$, similar to formula (15). Being rather cumbersome, it is omitted here.

A comparison of the calculation results shows that, at $\tau \ll T$, the $K_{\text{th}}(\tau)$ and $G^{(2)}(\tau)$ values practically coincide; therefore, formula (15) can also be used for estimated approximation of numerical simulation data. The ACF obtained as a result of numerical simulation at $\tau > Dq^2$ is also fairly close to that calculated from formula (15).

3. Correlation functions

In experimental measurements, the scattering region geometry depends on the light detection scheme; therefore, the functions determining the scattering region boundaries may differ from Gaussian (20). According to the data of [15], a replacement of a Gaussian dependence with a rectangular profile along one of the coordinates (z) does not lead to any qualitative changes in the time dependence of the ACF and is equivalent to the replacement of factor $2^{3/2}$ with 2 in the third term in (9); this circumstance gives grounds to interpret the experimental data on regions of a more complex shape within the theoretical model of the 'Gaussian' scattering region under consideration.

Figure 1 shows experimental correlation functions $G_{\text{exp}}^{(2)}(\tau)/B_{\text{exp}}(T)$, where

$$B_{\text{exp}}(T) = \left(\frac{1}{T} \int_0^T I(t) \mathrm{d}t \right)^2.$$

Experimental data were obtained for a monodisperse suspension of latex particles (with a radius of 375 nm) in water, using a system conventional for the DLS method [16], which makes it possible to measure the ACF of the light scattered at a specified angle. The light source was a 0.633-μm laser; the scatter-
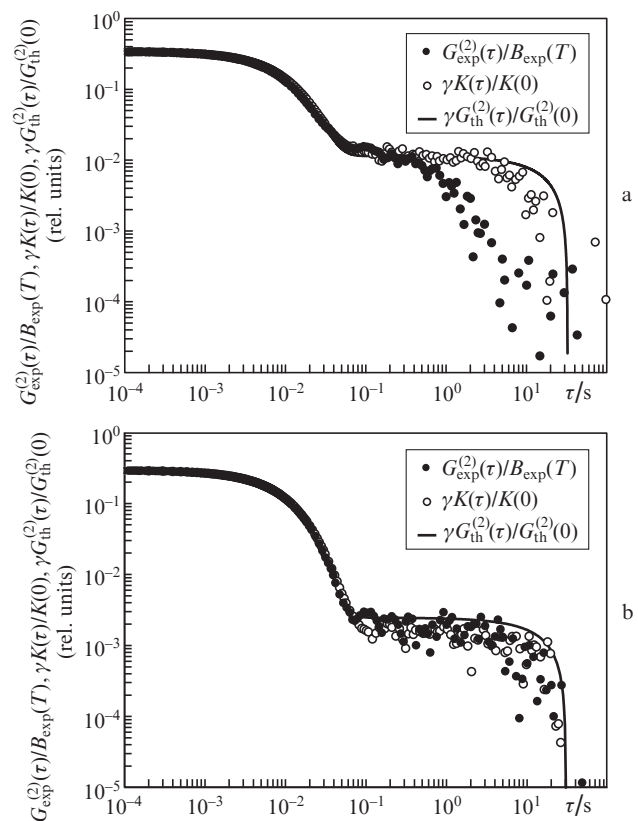
Figure 1. ACFs of the intensity of the light scattered at an angle $\theta = 40°$ for a monodisperse latex suspension ($R = 375$ nm) in water (measurement time $T = 100$ s): (filled circles) experimental ACFs measured at average numbers of particles in the scattering volume $\eta_{\text{exp}} =$ (a) 11 and (b) 36 and (open circles) ACFs calculated from the results of simulating an ensemble of Brownian particles in a Gaussian scattering volume with sizes $a = 150$ μm and $b = 90$ μm for $\eta =$ (a) 0.25 and (b) 1.1. The solid lines are the theoretical ACFs calculated from formula (15) for the aforementioned beam parameters a and b and the average numbers of particles $\eta_{\text{th}} =$ (a) 0.25 and (b) 1.1.

ing angle was taken to be $\theta = 40°$. The scattering region was formed by intersection of a Gaussian laser beam with the parameter $a = 150$ μm and a cylinder of radius $b_0 = 90$ μm (a round diaphragm installed before a photoelectron multiplier limited the scattering volume, whose image was projected by an objective onto the photoelectron multiplier cathode). The measurement time T was 100 s. Suspensions were prepared in carefully de-dusted cells of different geometries. The experimental results presented in Figs. 1a and 1b differ by the average number of particles, η_{exp}, in the scattering volume. Estimation of η_{exp} from the scattering intensity yields values of 11 and 36, respectively. Figure 1 shows also the results of calculating the intensity correlation functions $\gamma G_{th}^{(2)}(\tau)/G_{th}^{(2)}(0)$ in correspondence with formula (9) at $a = 150$ μm and $b = 90$ μm, along with the correlation functions $K(\tau)/K(0)$, obtained by computer simulation of the motion of an ensemble of a finite number of Brownian particles in a Gaussian beam having parameters $a_x = a_y = 150$ μm and $a_z = 90$ μm, with variation in the number N_p of particles (with radius $R = 375$ nm) in a modelled volume V, whose linear sizes were set to be $L_x = L_y = 10a$ and $L_z = 10b$. These $L_{x,y,z}$ values made it possible to use the model in a wide range of variation in parameters, proceeding from the condition of practical nullification of light beam intensity on the boundary of the simulation domain and from the condition of conserving (during simulation time T) the average particle concentration n in the scattering volume V_s; at long times, the concentration decreases as a result of particle diffusion beyond the simulation domain V. This condition can be formulated as $L_{x,y}/2\sqrt{8DT + a^2} \gg 1$. In the numerical calculations presented here, the duration of scattered light signals was limited to $T = 100$ s. For comparison with experimental data, the calculated correlation functions were multiplied by a factor $\gamma \sim 0.3$, which was controlled by the experimental conditions.

The data of Fig. 1 are indicative of satisfactory agreement between the results of computer simulation, calculation of the ACF from relation (15), and experimental measurements. For all these three groups of the results, the corresponding ratios of η values in Figs 1a and 1b are identical. Obviously, the difference of the absolute values of η_{exp} from the η values providing coincidence of the experimentally found and simulated ACFs may be due to the presence of a sharp boundary of the scattering region in the experiment, which is determined by the photodetector diaphragm. It can be seen that, for the number of particles in the modelled volume $N_p = 125$, which corresponds to the average number of particles in the scattering region, $\eta = 0.25$, the ACF values for $0.1 < \tau < 3$ s are an order of magnitude larger than for the η values exceeding 1.1 ($N_p = 570$); in this case, a descending portion arises in the range of $1 - 50$ s in Fig. 1. In addition, for the theoretical curves calculated at $\eta_{th} = 0.25$ and 1.1, one can select a descending portion in the range of $1 - 30$ ms, which corresponds to the correlation time $\tau_1 = 1/(2Dq^2)$. The values $N_p = 125$ and 570 correspond to volume particle concentrations of $n = N_p/(L_x L_y L_z) = 0.6 \times 10^5$ and 2.8×10^5 cm^{-3}, respectively. For $\eta \sim 0.1 - 1$, the ACF distortions at $\tau > 10/(2Dq^2)$ are caused by both the 'input–output' effect, which consists in the intersection of scattering volume boundary by Brownian particles (leading to modulation of scattering intensity) and the limited measurement (simulation) time. Under typical experimental conditions, $\tau_2 = a^2/(4D)$ is approximately an order of magnitude longer than the measurement time T; hence, at low particle concentrations in the suspension, for $\tau \ll \tau_2$, the sum of the third and fourth terms in the braces in

(15) is approximately constant and equal to $(4\sqrt{2}\eta)^{-1}(T/\tau_2)$. As a result, the $G_{th}^{(2)}(\tau)/G_{th}^{(2)}(0)$ and $K(\tau)/K(0)$ values in the range $10/(2Dq^2) < \tau \ll \tau_2$ are larger as compared with the case $\eta \gg 1$ [note that the second term in the braces in (15) can be neglected in this case]. With a further increase in τ, the effect of the particle 'input–output' from the scattering volume begins to manifest itself, and the third term in the braces in (15) decreases. The influence of these effects decreases with increasing particle concentration. The presence of two descending portions in the ACF should give rise to two modes in the reconstructed distributions of the scattered light intensity over particle sizes. One of these modes corresponds to particles with sizes of ~ 375 nm and correlation time $\tau_1 \sim 4$ ms, while the other mode corresponds to virtual particles with sizes more than ~ 0.1 mm. This effect (formation of an additional mode in the distribution) may occur when two conditions are satisfied: the length scale for the boundary of the scattering volume (Gaussian beam in our case) does not exceed the characteristic displacement of particles during the measurement time (i.e., the boundary should be sufficiently sharp), and the total number of particles in the scattering volume is small.

The characteristic time τ_3, at which (in the case of low concentrations) the second descending portion of ACF is observed, depends on the measurement time T and is determined by the time dependence of the sum of the third and fourth terms in the braces in (15). At the T values satisfying the condition $\tau_1 \ll T \ll \tau_2$, time τ_3 must be much shorter than τ_2, and, with an increase in the measurement time, the τ_3 values should tend to $a^2/(4D)$. If τ_3 is defined as the time at which the sum of the third and fourth terms in the braces in (15) is a half of this sum at $\tau = 0$, at T shorter than τ_2 (by an order of magnitude or more),

$$\tau_3 \approx \frac{T}{6}\left(1 + \frac{5}{24}\frac{T}{\tau_2}\right). \tag{23}$$

For example, at $a = 90$ μm and $R = 375$ nm, $a^2/(4D) = 2.8 \times 10^3$ μm, and at $T = 120$ s, $\tau_3 \approx 20$ s. In this case, the average 'particle radius' of the artefact mode amounts to 0.18 mm.

The finiteness of T, as well as the small number of particles in the scattering volume, cause ACF distortions, which may lead to underestimation of the correlation time for the fundamental mode and corresponding changes in the particle sizes (reconstructed from the measured ACF). At relatively short measurement times, satisfying the condition

$$\frac{1}{4\sqrt{2}\eta}\frac{T}{\tau_2} \ll 1,$$

the second term in (15), which is in essence a negative additive to the baseline, exceeds the sum of the third and fourth terms. When correlation function (15) is approximated by exponentials, this additive will result in underestimation of the correlation (decay) time of the fundamental mode. Using (15) and strong inequalities

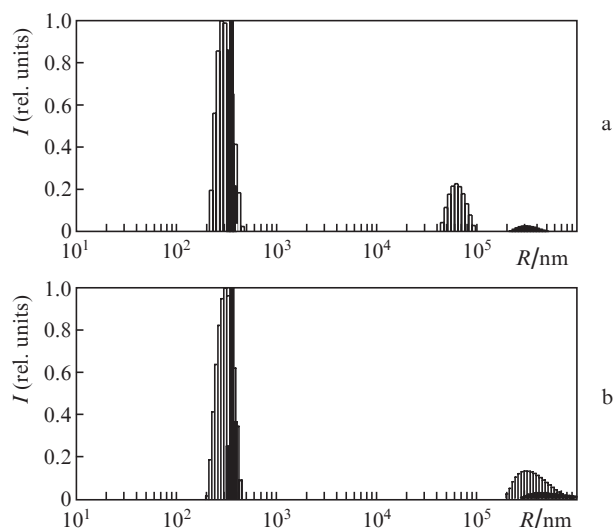$$\frac{2\tau_1}{T} \ll \frac{1}{4\sqrt{2}\eta}\frac{T}{\tau_2} \ll 1,$$

which are valid in our case, one can estimate the measured particle radius:

$$R_{meas} \approx R\left(1 + \frac{0.5\sqrt{(a^2 + 2b^2)DT}}{ab\eta}\right)^{-1}.$$

However, when carrying out a quantitative comparison with experimentally observed underestimations of particle radii, one must take into account that this estimate was obtained for the Gaussian model of the scattering region, which is characterised (in contrast to reality) by boundaries diffuse in all directions.

4. Particle size distributions

Figure 2 shows scattered light intensity distributions over particle sizes, obtained by expanding the ACF (see Fig. 1) in a sum of exponentials using a special computer programme DynaLS [17], which is based on histogram regularisation [18]. The occurrence of an artefact mode in the intensity distribution over particle sizes in DLS measurements is illustrated in Fig. 2a. The mode with a characteristic particle radius of 375 nm corresponds to latex particles. The measurements were performed in the concentration range from 2×10^5 to 2.9×10^6 cm^{-3} [6]; therefore, the average number of particles in a scattering volume of $\sim 1.2 \times 10^{-5}$ cm^3 is $2.5 - 35$; i.e., the condition for the Gaussian statistics of scattering intensity fluctuations is violated. In this case, an artefact mode (corresponding to the particles with radii of $0.1 - 1$ mm) arises; specifically this mode is observed experimentally (Fig. 2a). Note that the concentrations of particles and their number per scattering volume presented in the figures of [6] are overestimated. In this study, the scale of η_{exp} is refined based on the scattered light intensity. Note also that, in view of the incorrectness of the problem of reconstructing particle size distributions from measured ACFs, the experimental error in determining the baseline, and the smallness of ACF values at $\tau_1 < \tau \ll \tau_2$, the experimentally found sizes of the 'particles' corresponding to the artefact mode may differ significantly (by an order of magnitude or larger) from $R\tau_3/\tau_1$, where τ_3 is determined theoretically from (23). For comparison, Fig. 2b shows the scattered light intensity distributions over particle sizes that were reconstructed from ACFs; the ACFs were obtained by computer simulation of the motion dynamics for an ensemble of a finite number of Brownian particles. One can see in both figures that a decrease in the number of particles leads to broadening of the main peak in the distribution, shift of its maximum to smaller sizes, and increase in the artefact-mode fraction in the total intensity distribution over sizes. The latter two regularities were investigated experimentally by changing the suspension concentration.

Figure 3 shows the dependence of the artefact peak area A_2 (characterising its 'intensity') on the number of particles η_{exp} in the scattering volume V_s. In the series of experiments with solutions of different concentrations and constant scattering volume $V_s = 1.1 \times 10^{-5}$ cm^3, the peak area decreased proportionally to $1/\sqrt{\eta_{exp}}$.

$$A_2 = -0.058 + 0.88/\eta_{exp}^{1/2}$$
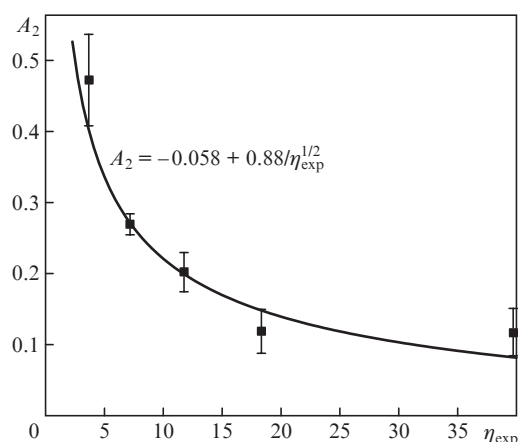
Figure 3. Dependence of the artefact peak area A_2 on the number of particles η_{exp} in the scattering volume; latex particle radius $R = 375$ nm, $\theta = 40°$.

The more pronounced the artefact peak (Fig. 4), the stronger the main peak in the histogram of the intensity distribution over particle sizes, which corresponds to the measured particle radius R_1, shifts to smaller sizes.
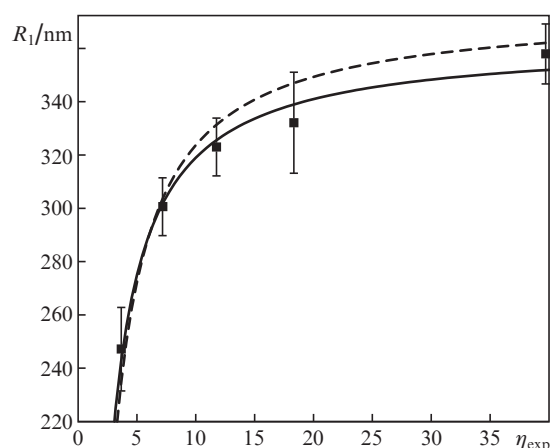
Figure 4. Dependence of the measured particle radius R_1 on the number of particles η_{exp} in the scattering volume; latex particle radius $R = 375$ nm (dashed line), $\theta = 40°$. The variable size R_0 (solid line) is commented in the text.

Figure 2. (a) Experimental and (b) calculated (based on the results of simulating the dynamics of an ensemble of Brownian particles) histograms of the distribution of the light intensity scattered by a suspension of latex particles with $R = 375$ nm in water at an angle $\theta = 40°$ over particle sizes; the histograms were obtained from the ACFs presented in Fig. 1 for small (open columns) and large (filled columns) numbers of particles in the scattering volume.

Early DLS studies with a small number of particles in the scattering volume revealed a change in the higher moments of the intensity distribution function [9, 19] or a distortion of the form of the correlation function (e.g., as a change in its baseline [8]) and, consequently, a distortion of the spectrum [14]; however, the artefact mode was not found in view of the imperfect equipment. The possible occurrence of this effect (when the number of particles in the scattering volume $\eta \sim 10$) is noted in the description of the Zeta-sizer (Malvern); there are also recommendations, according to which exact results can be obtained only when the number of particles η is no less than 500 [7]. Beginning with a certain concentration (individual for each particle size and each scattering angle), the dependence $R_1(\eta_{exp})$ tends to a constant value, close to the real particle size. This dependence was approximated by the formula $R_1(\eta_{exp}) = c/\eta_{exp} + R_0$, and the dependence $A_2(\eta_{exp})$ was approximated by the formula $A + B/\sqrt{\eta_{exp}}$. In the former case, the R_0 value was a fitting parameter (Fig. 4, solid line). In the latter case, it was assumed to be the real radius of latex particles: 375 nm (Fig. 4, dashed line). The approximation results are listed in Table 1.

Table 1. Results of approximating the dependences $A_2(\eta_{exp})$ and $R_1(\eta_{exp})$.

R_0/nm	A	B	c/nm	R_0/nm
375	-0.058 ± 0.046	0.88 ± 0.14	-512 ± 31	375
Variable value	–	–	-439 ± 31	361 ± 6

Apparently, these dependences can be explained as follows: the third term in the braces in expression (15) for $G_{th}^{(2)}(\tau)$ is proportional to η^{-1}, while the particle distribution is calculated using the program DynaLS, based on the expansion in decaying exponentials of the field correlation function $g^{(1)}(\tau) = \langle E(t)E^*(t+\tau)\rangle/\langle I\rangle$ on the assumption that it is related to $g_{exp}^{(2)}(\tau) = G_{exp}^{(2)}(\tau)/B(T)$ by the expression $g^{(1}(\tau) \sim \sqrt{g_{exp}^{(2)}(\tau)}$.

5. Conclusions

We have analysed the influence of the limited detection time and spatial distribution of laser beam intensity on the form of the intensity ACF for the light scattered by dispersed particles in a liquid. A computer simulation of the laser radiation scattering by an ensemble of Brownian particles of the corresponding size in dependence of their average number in the scattering volume has been performed to verify the theoretical relations derived for the ACF. The simulation results qualitatively confirm the conclusions of the theoretical analysis and are found to be consistent with the experimental data. It has been shown, both theoretically and experimentally, that the finiteness of the detection time at a small number of particles in the scattering volume leads to distortions of the correlation function, as a result of which the particle sizes reconstructed from the scattered-light intensity ACF are underestimated; the particle-size distribution becomes wider; and an artefact mode arises in the reconstructed distribution, which does not correspond to any particles that are actually present in suspension. It has been demonstrated experimentally that the measured particle radius decreases with decreasing number of particles in the scattering volume inversely proportionally to the number of these particles, while the artefact peak area decreases inversely proportionally to the square root of this number.

References

1. Xu R. *Particle Characterization: Light Scattering Methods* (Dordrecht, Netherlands: Kluwer Acad. Publ., 2000).
2. Berne B.J., Pecora R. *Dynamic Light Scattering* (Malabar, Florida: Krieger, 1990).
3. Skazka V.S. *Usp. Khim.*, **53** (5), 880 (1984).
4. Dhont J.K.G. *An Introduction to the Dynamics of Colloids* (Amsterdam: Elsevier, 1996).
5. Bunkin N.F., Shkirin A.V., Burkhanov I.S., Chaikov L.L., Lomkova A.K. *Quantum Electron.*, **44** (11), 1022 (2014) [*Kvantovaya Elektron.*, **44** (11), 1022 (2014)].
6. Kirichenko M.N., Sanoeva A.T., Chaikov L.L. *Bull. Lebedev Phys. Inst.*, **43** (6), 256 (2016) [*Kratk. Soobshch. Fiz. FIAN*, **43** (8), 32 (2016)].
7. *Zetasizer Nano Series. User Manual*. MAN0317 Issue 3.1 July 2007. Chapter 6. Sample Preparation (United Kingdom: Malvern Instruments Ltd., 2007) p. 6-3.
8. Schaefer D.W., Berne B.J. *Phys. Rev. Lett.*, **28**, 475 (1972).
9. Schaefer D.W., Pusey P.N. *Phys. Rev. Lett.*, **29**, 843 (1972).
10. Einshtein A., Smoluchowski M. *Braunovskoe dvizhenie* (Brownian Motion). Ed. by B.I. Davydov (Leningrad: ONTI, 1936).
11. Chapman S. *Proc. R. Soc. Lond. Ser. A*, **119**, 34 (1928).
12. von Smoluchowski M. *Bull. Intern. de l'Ac. De Sciences de Cracovie, A*, 418 (1913).
13. Cummins H.S., Pike E.R. (Eds) *Photon Correlation and Light Beating Spectroscopy* (New York: Plenum, 1974).
14. Voss R.F., Clarke J. *J. Phys. A: Math. Gen.*, **9** (4), 561 (1976).
15. Nijman E.J., Merkus H.G., Marijnissen J.C.M., Scarlett B. *Appl. Opt.*, **40** (24), 4058 (2001).
16. Kovalenko K.V., Krivokhizha S.V., Masalov A.V., Chaikov L.L. *Bull. Lebedev Phys. Inst.*, **36** (4), 95 (2016) [*Kratk. Soobshch. Fiz. FIAN*, **36** (4), 3 (2009)].
17. http://www.photocor.com/download/dynals/dynals-white-paper.htm.
18. Tikhonov A.N., Samarskii A.A. *Metody matematicheskoi fiziki* (Methods of Mathematical Physics) (Moscow: Nauka, 1977).
19. Schaefer D.W., Pusey P.N. *Statistics of Light Scattered by Non-Gaussian Fluctuations. In Coherence and Quantum Opt.* Ed. by L. Mandel et al. (New York: Plenum Press, 1973).